Chase, T., & Shaw, E. (1970) *Methods Enzymol. 19*, 20-27.
Crews, B. C., James, M. W., Beth, A. H., Gettins, P., & Cunningham, L. W. (1987) *Biochemistry 26*, 5963-5967.
Dangott, L. J., & Cunningham, L. W. (1982) *Biochem. Biophys. Res. Commun. 107*, 1243-1251.
Dangott, L. J., Puett, D., & Cunningham, L. W. (1983) *Biochemistry 22*, 3647-3653.
Davis, B. (1964) *Ann. N.Y. Acad. Sci. 121*, 404-427.
Downing, M. R., Bloom, J. W., & Mann, K. G. (1978) *Biochemistry 17*, 2649-2653.
Feldman, S. R., Gonias, S. L., & Pizzo, S. L. (1985) *Proc. Natl. Acad. Sci. U.S.A. 82*, 5700-5704.
Gettins, P. (1987) *Biochemistry 26*, 1391-1398.
Gettins, P., Beth, A. H., & Cunningham, L. W. (1988) *Biochemistry 27*, 2905-2911.
Gonias, S. L., & Pizzo, S. V. (1983) *J. Biol. Chem. 258*, 14682-14685.
Hall, P. K., & Roberts, R. C. (1978) *Biochem. J. 171*, 27-38.
Jensen, P. E. H., & Sottrup-Jensen, L. (1986) *J. Biol. Chem. 261*, 15863-15869.
Kẽzdy, F. J., & Kaiser, E. T. (1970) *Methods Enzymol. 19*, 14-20.
Laemmli, U. K. (1970) *Nature (London) 227*, 608-685.
Larsson, L.-J., & Björk, I. (1984) *Biochemistry 23*, 2802-2807.
Lee, D. C., & Chlebowski, J. F. (1988) *FASEB J. 2*, A347.
Pochon, F., & Bieth, J. G. (1982) *J. Biol. Chem. 257*, 6683-6685.
Roche, P. A., & Pizzo, S. V. (1987) *Biochemistry 26*, 486-491.
Sottrup-Jensen, L., Hansen, H. F., & Christensen, U. (1983) *Ann. N.Y. Acad. Sci. 421*, 188-208.
Sottrup-Jensen, L., Stepanik, T. M., Kristensen, T., Wierzbicki, D. M., Jones, C. M., Lønblad, P. B., Magnusson, S., & Petersen, T. E. (1984) *J. Biol. Chem. 259*, 8318-8327.
Steiner, J. P., Bhattacharya, P., & Strickland, D. K. (1985) *Biochemistry 24*, 2993-3001.
Strickland, D. K., Steiner, J. P., Migliorini, M., & Battey, F. D. (1988) *Biochemistry 27*, 1458-1466.
Thaler, E., & Schmer, G. (1975) *Br. J. Haematol. 31*, 233-243.
Travis, J., & Salvesen, G. S. (1983) *Annu. Rev. Biochem. 52*, 655-709.
Walsh, K. A., & Wilcox, P. E. (1970) *Methods Enzymol. 19*, 38-39.

Activation Energy of the Slowest Step in the Glucose Carrier Cycle: Break at 23 °C and Correlation with Membrane Lipid Fluidity†

Richard R. Whitesell,* David M. Regen, Albert H. Beth, Diana K. Pelletier, and Nada A. Abumrad
Department of Molecular Physiology and Biophysics, Vanderbilt University Medical School, Nashville, Tennessee 37232
Received December 20, 1988; Revised Manuscript Received March 16, 1989

ABSTRACT: Glucose transport in the rat erythrocyte is subject to feedback regulation by sugar metabolism at high but not at low temperatures [Abumrad et al. (1988) *Biochim. Biophys. Acta 938*, 222-230]. This indicates that temperature, which is known to alter membrane fluidity, also alters sensitivity of transport to regulation. In the present work, we have investigated a possible correlation between the effects of temperature on rate-limiting steps of glucose transport and on membrane fluidity. The dependences of methylglucose efflux and influx on cis and trans methylglucose concentrations were studied at temperatures between 17 and 37 °C. Membrane fluidity was monitored over the same temperature range by using electron paramagnetic resonance spectroscopy. External sugar did not affect efflux, and the K_m and V_{max} of sugar exit were respectively the same as the K_m and V_{max} of equilibrium exchange. These K_m's were relatively temperature independent, but the V_{max}'s increased sharply with temperature. The K_m and V_{max} of methylglucose entry were respectively much lower than the K_m and V_{max} of exit and exchange. Consistent with the above, intracellular sugar greatly enhanced sugar influx, and did so by increasing the influx V_{max} without affecting the influx K_m. Both lines of evidence indicated that the conformational change of the empty sugar-binding site from in-facing to out-facing orientation is the rate-limiting step of sugar entry into the rat erythrocyte. This was the case at all temperatures; however, the discrepancies of coefficients declined significantly with increasing temperature. The temperature dependence of the slowest step (change from in- to out-facing empty carrier) was evaluated. An Arrhenius plot showed that this step had a much greater activation energy below 23 °C than above: 48.5 ± 6.0 kcal/mol compared to 24.1 ± 1.8 kcal/mol. The temperature dependence of membrane fluidity, monitored by electron paramagnetic resonance spectroscopy of the probe 5-nitroxylstearate, also exhibited a transition near 23 °C. Our data indicate that membrane fluidity may be a factor influencing ease of carrier conformation change.

The relationship between the ordering of membrane lipids and the function of the membrane glucose carrier remains uncertain. In the human red blood cell (RBC), Lacko et al. (1973) showed a change in the activation energy for the glucose-entry V_{max} at around 20 °C. They suggested that the break could be related to the membrane structural transitions. Several such transitions have been documented (Forte et al., 1985). Lowe and Walmsey (1986) demonstrated a break in the Arrhenius plots of entry and exchange V_{max}'s for glucose transport at 35 °C, but without a change in the activation energy of the rate-limiting step of the carrier cycle. In the rat adipocyte, Amatruda and Finch (1979) compared the effect

† This work was supported by NIH Grant DK33301 and by Grants 18665 and 181563 from the Juvenile Diabetes Foundation.
* Author to whom correspondence should be addressed.

0006-2960/89/0428-5618$01.50/0

of temperature on the fluidity of purified plasma membranes to that on sugar transport in intact cells. Multiple breaks were observed in the Arrhenius plots of transport activity and membrane fluidity. More recent findings document glucose transport heterogeneity in adipocytes.[1] Also, gradual effects of temperature on transport kinetics are possible (Ezaki & Kono, 1980), demonstrating the need for a simple cell system for studies of this kind.

In order to reassess the correlation between membrane lipid ordering and glucose transport function, a cell type which is relatively homogeneous and stable with respect to transport characteristics is advantageous. In addition, transport rates should be slow enough so that time courses include initial rate measurements at all temperatures tested. We have previously shown that the rat red blood cell equilibrates with sugar slowly compared to human RBC and is quite stable compared to the rat adipocyte (Abumrad et al., 1988). In this study, we have analyzed glucose transport kinetics of the rat erythrocyte over a wide range of temperatures. We have compared the temperature dependence of the rate-limiting step in the carrier cycle with that of membane lipid fluidity studied over the same temperature range.

Materials and Methods

Incubation Medium. Medium was a Hepes-buffered Krebs salt solution containing 0.2% bovine serum albumin at pH 7.5, as described earlier (Abumrad et al., 1988). Stock solutions of the salts were prepared fresh each week and were stored at 4 °C. They were added to water on the day of each experiment. The water used was deionized and then glass distilled.

Preparation of RBC. The rats were anesthetized by intraperitoneal injection with nembutal. Blood (about 10 cm^3) was collected by aortic puncture using a heparinized syringe. The blood was diluted with 3 volumes of normal saline at room temperature and layered over Percoll (Pharmacia) made isotonic with NaCl (density 1.04 g/mL). The cell pellet, obtained by centrifugation in a clinical centrifuge for 10 min at medium speed, was washed twice with incubation medium and then diluted to about 7% hematocrit. Cells were depleted of intracellular glucose by incubation with shaking at 37 °C for two consecutive 20-min periods separated by a change of medium. This regimen has been shown to reduce intracellular glucose concentration to the low micromolar range (Abumrad et al., 1988). The cells were then resuspended in fresh medium to a 40% hematocrit, and aliquots were added to round-bottomed 50-mL polycarbonate tubes. An equal volume of incubation medium containing twice the desired concentration of "preloading" sugar was added at this point, and the suspension was incubated with shaking at 37 °C for 1 h. For efflux experiments, the preloading sugar was [^{3}H]methylglucose (New England Nuclear, Boston, MA) dried under N_2 from an ethanol solution at room temperature with unlabeled methylglucose added to yield 1 or 20 mM and about 1000 cpm/μL.

Efflux Measurements. RBC (containing 1 or 20 mM [^{3}H]methylglucose) and media were warmed (about 10 min) to the stated temperature by immersion of the incubation tubes in a slowly shaking water bath. Three hundred microliters of cell suspension was then added with swirling to 12 mL of efflux medium, which was incubation medium containing a stated concentration of unlabeled methylglucose. The suspension was incubated with constant swirling. Temperature

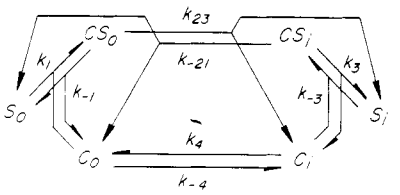

FIGURE 1: Mobile carrier model. The labeled arrows denote steps which comprise parts of the glucose transport cycle as referred to in the text. The branching arrows as part of the model have been discussed (Regen & Tarpley, 1974) and make the model simpler than the complete iso–uni–uni model (Segel, 1975) without changing the solution.

was monitored by a thermometer placed in an adjacent test tube during the study and was stable ±0.5 °C. Sampling for remaining intracellular radioactivity was accomplished by withdrawing 1.5 mL from the incubation at the desired time and adding it with swirling to 3 mL of ice-cold incubation medium without albumin and containing 100 μM phloretin (stop solution). This tube was kept on ice and centrifuged within 10 min in an IEC centrifuge at 4 °C at full speed setting for 3 min. The supernatant was aspirated without disturbing the pellet, and 2 mL of additional stop solution was added to rinse down the sides of the tube and resuspend the pellet. The tubes were then centrifuged and processed as before. Ice-cold water (500 μL) was added with vortexing to lyse the cells, and then 500 μL of ice-cold 1 M perchloric acid was added to precipitate the hemoglobin. The tubes were centrifuged once more, and 700 μL of the clear supernatant was added to vials containing 7 mL of aqueous scintillation fluid for counting.

The data were analyzed by the SAS procedure NLIN (Carey, NC) with the resulting curve fits and statistics shown in the figures. The initial rates of efflux at two differing concentrations were used in computing the efflux K_m's.

Influx Measurements. Preloaded cells were reconcentrated to 60%, keeping the final preloading concentration of methylglucose constant, and kept on ice until the transport assay when they were warmed to the stated temperatures. Aliquots (200 μL) of [^{3}H]methylglucose solutions at the desired concentrations were pipetted into 15-mL tubes at the same temperature. Influx was started by addition of 40 μL of cell suspension to isotope solutions with swirling. To terminate, 3 mL of stop solution was added, and the tubes were placed on ice and processed as described for the efflux experiments.

The data were plotted as $(cpm - cpm_0)/(cpm_\infty)$ versus time. The expression $[S_i]/[S_o]$, where S_i is internal sugar and S_o is external, is equivalent. cpm_0 was obtained by extrapolation of the time course plot to zero time. In this case, cpm_0 was the counter blank plus the contribution from extracellular radioactivity. The cpm_0 obtained from cells to which stop solution was added before the isotope closely approximated the value obtained from the time course plots. cpm_∞ was calculated as the radioactivity in the cells at equilibrium, assuming 80% of the packed cell volume to be accessible to the sugar. This corresponded closely to the value obtained for cells equilibrated 1 h with tracer methylglucose at 40 °C. Sampling times were planned so that cpm was at most 20% of cpm_∞. The first-order rate constant was obtained from a best fit according to a negative exponential model.

Evaluation of Empirical Transport Coefficients. If the glucose transporter has only one sugar-binding site which alternately faces the external and internal compartments (Figure 1), then all transport phenomena in the presence of one kind of sugar can be accounted for with the following rate law (Regen & Morgan, 1964; Regen & Tarpley, 1974; Whitesell et al., 1977a):

[1] R. R. Whitesell, D. M. Regen, and N. A. Abumrad, submitted for publication.

$$\nu_s = \frac{F_s[S_o](1 + [S_i]/R_s) - F_s[S_i](1 + [S_o]/R_s)}{1 + [S_o]/K_{so} + [S_i]/K_{si} + [S_o][S_i]/R_sB_s} \quad (1)$$

F_s is an activity coefficient, the rate coefficient for influx or efflux if sugar concentration is very low. K_{so}, K_{si}, and B_s are Michaelis coefficients for entry, exit, and equilibrium exchange, respectively. R_s is the concentration of sugar on one side which reduces the cis/trans ratio of empty carrier by half. The four coefficients are related:

$$1/B_s + 1/R_s = 1/K_{so} + 1/K_{si} \quad (2)$$

Thus, there can be four independent coefficients: the activity coefficient (F_s) and three of the four half-saturation coefficients as dictated by relation 2. Unidirectional influx (ν_{s+}) is represented by the first term in the numerator of eq 1, $F_s[S_o](1 + [S_i]/R_s)$, divided by the denominator; and unidirectional efflux (ν_{s-}) is the second numerator term, $F_s[S_i](1 + [S_o]/R_s)$, divided by the denominator. For net transport, eq 1 can be written with a much simpler numerator, $F_s([S_o] - [S_i])$.

The product of F_s and a half-saturation coefficient is a V_{max}. There are four V_{max}'s, three of which are independent: entry V_{max} or $V_{so} = F_sK_{so}$; exit V_{max} or $V_{si} = F_sK_{si}$; equilibrium exchange V_{max} or $V_{sb} = F_sB_s$; rate of empty carrier exchange in the absence of sugar or $V_{sr} = F_sR_s$.

Under conditions where sugar is present only on one side of the membrane, F_s and K_{so} can be evaluated from the dependence of the initial entry on $[S_o]$, and F_s and K_{si} can be evaluated from the dependence of the initial exit on $[S_i]$. Under equilibrium exchange conditions (sugar concentration is the same on both sides of the membrane), F_s and B_s can be obtained from measurements of influx or efflux at various equilibrium sugar concentrations. In each case, when the data are plotted as concentration/rate versus concentration, F_s is the reciprocal of the y intercept, and K_{si}, K_{so}, or B_s is the absolute value of the x intercept. R_s can then be estimated from K_{si}, K_{so}, and B_s by eq 2.

All empirical coefficients can be evaluated in a single experiment with one kind of measurement (Whitesell et al., 1977a). Initial tracer influx (ν_{s+}) is measured at various external sugar concentrations ($[S_o]$) with initially no internal sugar ($[S_i]$) and also with a substantial $[S_i]$. In the absence of internal sugar, the y and x intercepts of the $[S_o]/\nu_{s+}$ versus $[S_o]$ plot yield F_s and K_{so}, respectively. The y intercept of this plot is the point where $[S_o] = [S_i] = 0$. One point on the other plot (with constant $[S_i]$ initially) is where $[S_o] = [S_i]$ at a finite concentration of sugar. A straight line drawn between these two points will allow evaluation of the exchange K_m or B_s which would be the x intercept. With K_{so} and B_s evaluated, R_s can be evaluated from any of the three key features of the $[S_o]/\nu_{s+}$ versus $[S_o]$ plot with substantial $[S_i]$, namely, the x intercept, the y intercept, or the slope. For example, R_s can be calculated by the formula:

$$R_s = [S_i]\frac{1 - H_s/B_s}{([S_i] + H_s)/K_{so} - (1 + [S_i]/B_s)} \quad (3)$$

where H_s is the influx K_m in the presence of the constant $[S_i]$. With K_{so}, B_s, and R_s known, K_{si} can be evaluated by eq 2.

Estimation of Coefficients for the Steps in the Transport Cycle. Each of the V_{max}'s discussed previously is proportional to the total amount of transporter present, C_t, and to the conductance through two steps in series as can be seen from Figure 1. The conductance through two steps is the reciprocal of the sum of the reciprocals of the two conductances. The two steps involved in net entry (Figure 1) are k_{23} (from CS_o to $C_i + S_i$) and k_4 (from C_i to C_o); so

$$1/V_{so} = (1/k_{23} + 1/k_4)/C_t \quad (4a)$$

The two steps involved in net exit are k_{-21} (from CS_i to $C_o + S_o$) and k_{-4} (from C_o to C_i); so

$$1/V_{si} = (1/k_{-21} + 1/k_{-4})/C_t \quad (4b)$$

The two steps involved in equilibrium exchange are k_{23} (from CS_o to $C_i + S_i$) and k_{-21} (from CS_i to $C_o + S_o$); so

$$1/V_{sb} = (1/k_{23} + 1/k_{-21})/C_t \quad (4c)$$

The two steps involved in exchange of empty carrier are k_4 (from C_i to C_o) and k_{-4} (from C_o to C_i); so

$$1/V_{sr} = (1/k_4 + 1/k_{-4})/C_t \quad (4d)$$

Therefore, evaluation of the V_{max}'s allows the determination of the relations among the step coefficients of the model.

Since only three of the V_{max} values of eq 4 are independent, eq 4a–d does not provide for a unique solution of step coefficients. Relations among the possible kC_t values are conveniently shown in a plot of each $1/kC_t$ against $1/k_4C_t$, a so-called "resistance plot". The corresponding values are calculated as

$$1/k_{23}C_t = 1/V_{so} - 1/k_4C_t \quad (5a)$$

$$1/k_{-21}C_t = 1/V_{sb} - 1/k_{23}C_t \quad (5b)$$

$$1/k_{-4}C_t = 1/V_{sr} - 1/k_4C_t \quad (5c)$$

Since no resistance can be less than zero, the plot places an upper and lower limit on each $1/kC_t$. Further interpretation of V_{max}'s requires an assumption—that kC_t values which might be similar are similar, or that each k increases with temperature, or that the activation energies are constant.

One can also calculate dissociation constants from empirical constants and step coefficients. The dissociation constant of out-facing carrier is defined and calculated $K_{sdo} = (k_{-1} + k_{23})/k_1 = R_sk_{23}/k_{-4}$; the dissociation constant of in-facing carrier is defined and calculated $K_{sdi} = (k_3 + k_{-21})/k_{-3} = R_sk_{-21}/k_4$.

EPR Studies. Washed rat erythrocytes were spin-labeled with 5-[^{15}N]nitroxylstearate (^{15}N-5-NS) as follows. An aliquot (10 μL) of a 2 mM stock of ^{15}N-5-NS in ethanol was dried on the walls of a test tube. Erythrocytes, 1 mL of a 50% hematocrit suspension in 5 mM sodium phosphate/0.15 M sodium chloride, pH 7.4, were added to the tube and incubated for 5 min at 37 °C. EPR spectra were recorded with a Varian E-109 spectrometer operating at X-band microwave frequency. Samples were introduced into the E-238 cavity in a WG-812 flat cell (Wilmad). Samples were maintained at the desired temperature (±0.5 °C) with an E-257 variable-temperature accessory by blowing precooled air directly into the cavity through the front optical port. Spectra were recorded using a 100-kHz Zeeman field modulation of 1.0-G amplitude at a microwave power setting of 10 mW. A PDP 11/03 microcomputer was used to drive the spectrometer's magnetic field sweep and to record signals digitally. Order parameters (S) for membrane-associated ^{15}N-5-NS were determined from experimental spectra recorded at the indicated temperatures using the relationship:

$$S = (A_\parallel^e - A_\perp^e)/(A_\parallel^c - A_\perp^c) \quad (6)$$

where $A_\parallel^e$ and $A_\perp^e$ are the separations (in Gauss) between the major and minor element spectral structurings measured from the experimental spectrum, respectively, and $A_\parallel^c$ and $A_\perp^c$ are the values for these same splittings for the case $S = 1$. Values for these latter splittings were calculated from those reported

Table I: Characteristics of Equilibrium Exchange of Methylglucose Measured as Efflux, and Inhibition by Cytochalasin B[a]

	14 °C (n = 5)	40 °C (n = 7)
B_s (mM)	11.6 ± 3.2	15.5 ± 2.6
V_{sb} [μM/(mL·min)]	0.10 ± 0.02	2.16 ± 0.62
K_i(cB) (1 mM MeGlc) (μM)		2.8 ± 0.52
K_i(cB) (20 mM MeGlc) (μM)		12.7 ± 2.43

[a] The data are from efflux experiments such as shown in Figure 2. Efflux rates at 1 and 20 mM MeGlc were obtained by regression analysis of six different time points at each concentration. K_m and V_{max} were then calculated, and the standard error of the mean was given for n determinations. Where the values are shown at 40 and 14 °C, paired experiments were performed on the same cells. The values for the half-maximal inhibitory concentration of cytochalasin B [K_i(cB)] were determined by regression of efflux curves with 0, 0.2, and 3 μM cytochalasin B at 1 and 20 mM MeGlc at 40 °C. In these cases, the standard deviation of the least-squares regression is given.

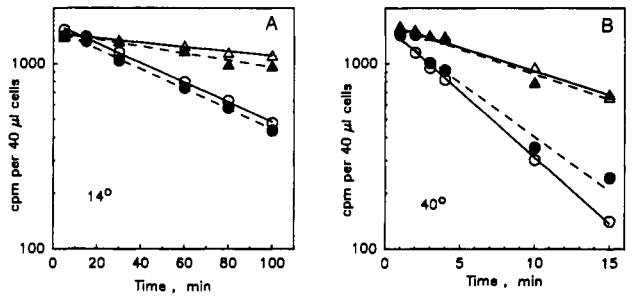

FIGURE 2: Efflux of methylglucose with low and high external methylglucose concentrations. (Panel A) Data from an efflux experiment at 14 °C. Cells loaded with 1 mM (○, ●) or 20 mM (△, ▲) radioactive MeGlc were diluted in medium to give an external concentration of 1 mM (○, △) or 20 mM (●, ▲). (Panel B) Data from an experiment at 40 °C. The symbols have the same meaning as in panel A. The data shown are representative of three experiments. The effects of temperature (panel A vs panel B) and the effects of internal sugar concentration (△ vs ○) were statistically significant, but effects of external sugar concentration (closed vs open symbols) were not.

for ^{14}N-5-NS (Gaffney, 1976) by multiplying by 1.4 to correct for differences in gyromagnetic ratios for the ^{15}N and ^{14}N nitroxide nitrogen nuclei.

Results

Inhibition by Cytochalasin B. To demonstrate that the fluxes measured were carrier mediated, a series of experiments was employed to characterize the effect of cytochalasin B on methylglucose efflux and influx. Results for efflux are summarized in Table I. Efflux of 1 mM methylglucose was inhibited 50% by 2.8 μM cytochalasin B. Inhibition appeared to be competitive in that efflux of 20 mM sugar was much less affected by cytochalasin B, K_i being about 12.7 μM.

Influx was also inhibited by cytochalasin B, K_i being 1–2 μM (data not shown). A residual transport component was observed which was insensitive to inhibition by either cytochalasin or phloretin or by the combination of both inhibitors. The cytochalasin-insensitive influx was subtracted from the total influx before further analysis (evaluation of kinetic parameters and their temperature dependencies). The data presented were corrected this way. However, analyses of uncorrected data were very similar as regards kinetic parameters and their temperature dependences, so this refinement was of little consequence.

Efflux with Low and High External Sugar Concentration. Figure 2A is a plot of radioactivity remaining in cells preequilibrated with 1 and 20 mM labeled methylglucose and then diluted 20-fold in medium at 14 °C containing 1 and 20 mM unlabeled sugar. Figure 2B is an analogous experiment at 40 °C. The sampling times were appropriate for defining the rate

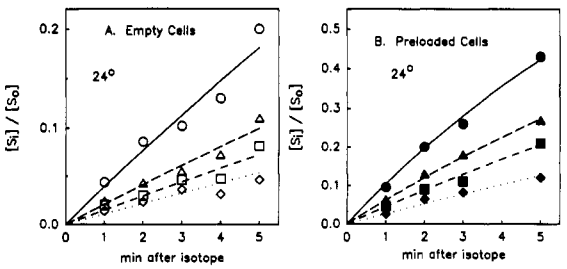

FIGURE 3: Time courses of methylglucose influx at various sugar concentrations. The data shown are a composite from three experiments at 24 °C. Panel A shows time courses of uptake of four different concentrations of MeGlc into cells initially lacking sugar. Going from the top curve to the bottom curve, the external concentrations were 0.46 (○), 2.31 (△), 4.63 (□), and 9.26 mM (◇). Panel B shows the data for cells which were preloaded with 10 mM MeGlc, for which the concentrations of labeled sugar at the start of uptakes were 0.89 (●), 3.05 (▲), 5.37 (■), and 10.0 (♦) mM going from top to bottom. The curves fitting the data are the outcome of the statistical treatment described under Materials and Methods. The standard deviations of the fits are shown in Figure 4. Experiments of this kind were performed at many different temperatures.

at each temperature. The rate of efflux at both temperatures was independent of external sugar concentration. No "trans effect" of external sugar was observed.

Combining efflux data from cells loaded and diluted in 1 mM sugar with data from cells loaded and diluted in 20 mM sugar, we estimated kinetic parameters of equilibration exchange (B_s, V_{sb}). As seen in Table I, B_s (exchange K_m) was similar at 14 and 40 °C, whereas V_{sb} (exchange V_{max}) increased about 20-fold between 14 and 40 °C. Since external sugar did not affect efflux at either temperature, we can conclude that K_{si} (exit K_m) was about 12–16 mM at both temperatures and V_{si} (exit V_{max}) increased about 20-fold with the temperature increase.

Testing for Multiple-Site Interaction between Carrier and Substrate. In contrast to the foregoing results with efflux, sugar influx exhibits a large trans effect in rat (Abumrad et al., 1988) and human (Lacko et al., 1973; Hankin & Stein, 1972; Lowe & Walmsey, 1986) erythrocytes, with internal sugar enhancing influx substantially. The prominent trans effect and its sidedness indicate a very asymmetric interaction of sugar with its transporter. Such interaction could occur through binding of the sugar to the transport site itself, promoting reorientation to the outside. On the other hand, binding could occur to another, separate site on the glucose carrier or even to an associated molecule. The latter possibilities would constitute multiple-site interactions of the carrier with the sugar and should be manifest in a sigmoidal dependence of efflux or equilibrium exchange on sugar concentration, i.e., in a bent Hanes plot. We examined equilibrium exchange of external labeled sugar with internal unlabeled sugar rather exhaustively to test for this possibility. Statistical treatment of the Hanes plot revealed very good fit to a straight-line function. Thus, there was no evidence for interaction of internal sugar with other than the transport site itself.

Measurement of Zero-Trans and Trans-Loaded Influx. The previous data established several useful facts: (a) there is no detectable trans effect of external sugar, (b) the efflux K_m (K_{si}) is identical with the exchange K_m (B_s), at the temperatures tested, (c) B_s and K_{si} are not very temperature sensitive while V_{si} and V_{sb} are, and (e) the dependence of exchange on sugar concentration is a simple function which can be characterized from measurments at two concentrations. To investigate the temperature dependence of uptake and the influence of internal sugar, influx saturation was tested at

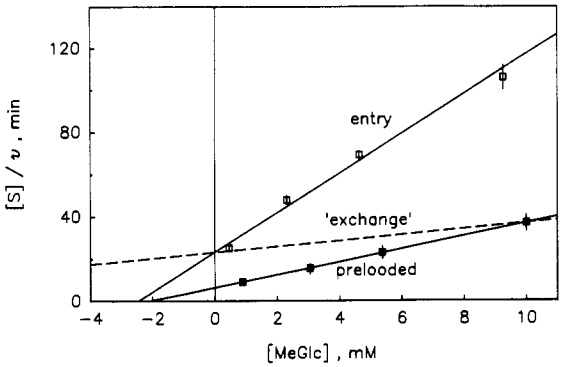

FIGURE 4: Hanes plot of the data of Figure 3. The upper curve plots the reciprocals of the fractional clearances from panel A of Figure 3 as open squares, and the lower curve corresponds to panel B. The data were corrected by subtracting the component of transport which was insensitive to cytochalasin B. The data show the limits of the standard errors of the values resulting from the curve fits shown in Figure 3. The dashed line was drawn to connect the two points which characterize the saturation kinetics of equilibrium exchange, one at the y intercept where concentration was 0 mM and another at 10 mM. This is justified from the strictly linear S/v vs S relation of equilibrium exchange.

various temperatures without and with a fixed internal sugar concentration. Figure 3 shows the data obtained at 24 °C. Figure 3A shows time courses of radioactive sugar uptake by cells initially lacking sugar. Figure 3B shows time courses of radioactive sugar influx into cells initially containing 10 mM methylglucose. This experiment was repeated at many temperatures.

Figure 4 is a Hanes plot of the data from Figure 3. This plot has been described previously (Whitesell et al., 1977a). The x intercept of the dashed line between the two points as $[S_o] = [S_i] = 0$ and $[S_o] = [S_i] = 10$ mM gives B_s, the exchange K_m. Because these two points are well-defined and the line between them was demonstrated to be straight (not shown), the exchange K_m (B_s) is evaluated with good precision. The y intercept of the $[S_o]/v_{s+}$ vs $[S_o]$ plot with no internal sugar is $1/F_s$, the reciprocal of the activity constant. The y intercept of the $[S_o]/v_{s+}$ vs $[S_o]$ plot with a fixed internal sugar concentration is $1/P_s$, P_s being the apparent activity constant for the condition. The x intercept with no internal sugar gives K_{so}, the entry K_m. The x intercept with fixed internal sugar concentration gives H_s, the apparent K_m for the condition. These values allow the calculation of the other constants. As it turned out, H_s and K_{so} were not statistically different, indicating that R_s was not statistically different from K_{so} (eq 3) and that K_{si} was not statistically different from B_s (eq 2). This confirms the previous results obtained with the efflux experiments of Figure 2 (showing $B_s = K_{si}$).

Estimation of Step Constants. Figure 5 displays the combinations of step rate constants (in reciprocal) and dissociation constants compatible with the empirical coefficients of one experiment. We call this a "resistance plot" because reciprocal rate constants are resistances. The vertical dotted lines mark the range of possible $1/k_4C_t$ values, below which $1/k_{-21}C_t$ would be negative (impossible) and above which $1/k_{-4}C_t$ and $1/k_{23}C_t$ would be negative (impossible). Because outward reorientation of empty carrier is the rate-limiting step, its rate constant (k_4C_t) is defined within narrow, finite limits, while the other rate constants might be anywhere between lower limits and infinity. The value of k_4C_t midway in the range of possible values is not very different from its value at either extreme, so the mid-range value is accurately representative. It appears from the very low value of k_4C_t that some factor stabilizes the in-facing empty carrier.

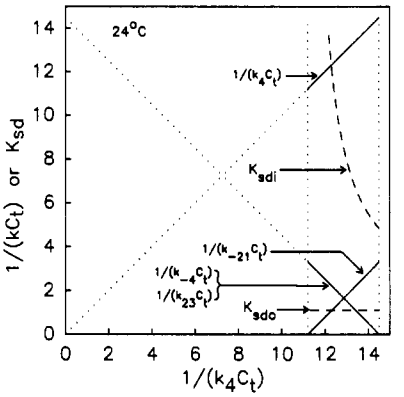

FIGURE 5: Resistance plot showing relations among step coefficients of the transport cycle consistent with empirically determined transport parameters. These relations were derived as described under Materials and Methods from one of the experiments at 24 °C as an example of the operation which was performed for all experiments. The possible values for the rate coefficients lie between the vertical dotted lines. The dimensions of kC_t are micromoles per minute per milliliter of cell water; that of K_{sd} is millimolar. At the extreme denoted by the right dotted line, $1/k_{-4}C_t = 0$, which means that k_{-4} is infinity since C_t is a constant. It then follows that $k_4/k_{-4} = 0$ or $14.5/\infty = 0$. At the extreme denoted by the left dotted line, $1/k_{-4}C_t = 3.3$ and $1/k_4C_t = 11.2$; so the ratio of k_4/k_{-4} is 0.30.

Table II: Summary of Kinetic Coefficients Determined from 17 to 37 °C[a]

temp (°C)	H_s, K_{so}, R_s (mM)	K_{si}, B_s (mM)	F_s (min^{-1})
37	4.0, 2.7	7.8, 5.4	0.100, 0.135
35	2.2	5.0	0.111
34	1.5, 2.8, 1.4	4.1, 7.6, 11.3	0.128, 0.105, 0.181
32	1.7	4.4	0.09
29	2.4, 2.1, 1.2	7.6, 7.2, 3.4	0.063, 0.065, 0.091
27	2.0, 1.6	9.3, 7.9	0.051, 0.053
26	2.0, 1.0	7.5, 4.2	0.056, 0.080
24	1.9, 1.8, 1.8, 1.1	10.0, 13.7, 5.9, 4.8	0.035, 0.039, 0.044, 0.063
22	1.3, 0.7	10.7, 2.4	0.032, 0.056
21	1.1, 1.2, 2.0, 1.1	6.2, 5.0, 12.5, 7.0	0.025, 0.033, 0.025, 0.029
19	0.7, 0.8	4.9, 6.2	0.024, 0.025
18	0.8	5.9	0.018
17	0.35, 0.8, 0.65, 0.60	3.6, 5.2, 10.7, 3.9	0.019, 0.018, 0.013, 0.018

[a] The results from all the experiments within the range of temperatures tested between 17 and 37 °C are shown. Calculation of the values shown and subsequent computation of k_4C_t and other coefficients are described under Materials and Methods.

The dissociation constants (K_{sdo}, K_{sdi}) compatible with the various half-saturation constants (K_{so}, K_{si}, B_s, R_s) and the step coefficients (kC_t) are shown as dashed lines. Because inward reorientation of the carrier is indifferent to loading ($k_{23} = k_{-4}$), the entry K_m (K_{so}) and the counterflow K_m (R_s) are the same as the external dissociation constant (K_{sdo}), which in this experiment was about 1 mM. For the same reason, the exit K_m (K_{si}) and the exchange K_m (B_s) are the same, but because loading promotes outward reorientation ($k_{-21} > k_4$), these half-saturation constants are less than the internal dissociation constant (K_{sdi}). Thus, the asymmetry of Michaelis constants ($K_{si} \gg K_{so}$) is due entirely to the asymmetry of dissociation constants ($K_{sdi} \gg K_{sdo}$). From this, it appears that some factor interferes with loading of in-facing empty carrier.

The resistance plot analysis was applied to all experiments of the kind illustrated in Figures 3 and 4, carried out at temperatures between 17 and 37 °C. At all temperatures, the picture was as seen in Figure 5—outward reorientation of empty carrier was the rate-limiting step, so k_4C_t was well-

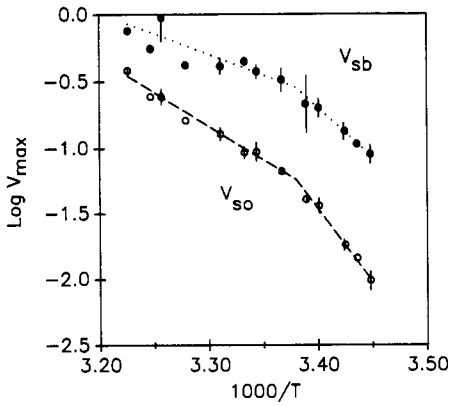

FIGURE 6: Temperature dependence of V_{so} and V_{sb}. Arrhenius plots of V_{so} and V_{sb} are shown. The dimensions of V_{max} are micromoles per minute per milliliter of cell water; that of T is degrees absolute temperature. The line fits shown were drawn by piecewise linear regression with the data grouped to either side of the break point 3.38 (22.8 °C). The slope, whose absolute value was proportional to the activation energy, was −5.56 ● 0.29 to the left of the breakpoint and −11.59 ± 1.11 to the right, with $r^2 = 0.98$. For V_{sb}, the slope was −2.45 ± 0.49 to the left and −5.23 ± 1.33 to the right of the break point, $r^2 = 0.87$.

Table III: Activation Energies (kcal/mol)[a]

	above 23 °C	below 23 °C
k_4	24.1 ± 1.8	48.5 ± 6.0
V_{so}	23.8 ± 1.5	51.1 ± 5.4
V_{sb}	11.2 ● 2.2	34.1 ± 8.3
K_{so}[b]	9.1 ± 1.4	
B_s[b]	−2.5 ± 1.4	

[a] Activation energies were calculated from the slopes and intercepts given in Figure 6 for V_{so} and V_{sb}, and in Figure 7 for k_4. Standard errors were calculated from the statistical variances obtained by piecewise linear regression of the data. [b] K_{so} and B_s were plotted as log K_m vs $1000/T$. One slope only was evident in the temperature range from 17 to 37 °C. Since the parameters were not rates, the slopes in this case do not represent activation energies.

defined; the dissociation constant of in-facing carrier substantially exceeded that of out-facing carrier.

Temperature Dependence of Kinetic Coefficients. Table II shows empirical kinetic coefficients estimated at many temperatures between 17 and 37 °C. It is seen that the activity constant (F_s) increased about 8-fold as temperature increased over this 20 °C range. The entry K_m (K_{so}) and the counterflow K_m (R_s) increased about 5-fold with the 20 °C increase of temperature. The exit K_m (K_{si}) and equilibration–exchange K_m (B_s) varied widely at all temperatures and exhibited no temperature dependence.

Although the carrier has four distinct V_{max}'s (products of F_s and the four K_m's), there were only two different V_{max} values, i.e., $V_{so} = V_{sr}$ and $V_{si} = V_{sb}$. Their temperature dependences are shown in Figure 6 as Arrhenius plots. Each of these temperature dependences shows a discontinuity near 23 °C ($1000/T = 3.38$). Activation energy below the discontinuity was much greater than that above the discontinuity, as summarized in Table III. Since all V_{max}'s exhibited the transition, we conclude that at least two of the step coefficients exhibit the transition, and we suspect that they all do.

As shown in Figure 5, outward reorientation of empty carrier (k_4) was the rate-limiting step of glucose entry. Its conductance (k_4C_t) was, therefore, estimated with good precision at all temperatures. As seen in Figure 7, the Arrhenius plot of k_4C_t is very similar to that of V_{so} and V_{sr} as regards height, slopes, and transition temperature. Thus, at least one step demonstrably has a much lower activation energy above 23 °C than below 23 °C.

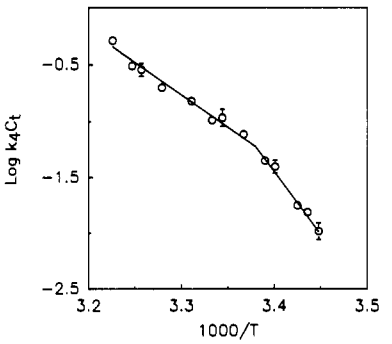

FIGURE 7: Temperature dependence of k_4C_t. An Arrhenius plot of k_4C_t is shown. For dimensions, see Figures 5 and 6. The conductances were calculated from the data of Table II by eq 5, and the values shown represent the midpoint between the limits. The discontinuous fits were generated as in Figure 6 ($r^2 = 0.98$). The slope was −5.28 ± 0.38 in the interval of $1000/T$ from 3.225 to 3.38 and −10.85 ± 1.29 in the interval from 3.38 to 3.45.

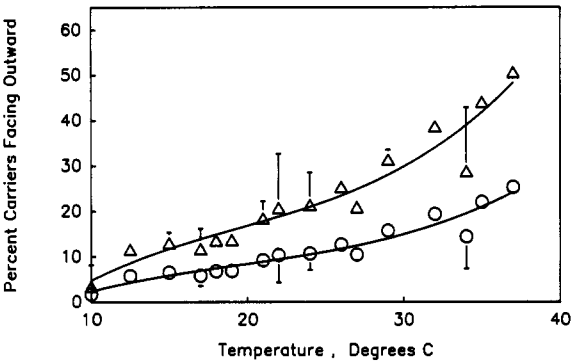

FIGURE 8: Effect of temperature on the distribution of empty transporter sites between inward and outward orientations. The lower line (○) shows points calculated from the k_4/k_{-4} ratio in the middle of the possible range of values for k_4 (where $k_{-21} = k_{23} = k_{-4}$). The upper line (△) shows points calculated at the lowest possible k_4 (left dotted line of Figure 5, where $k_{-21} >>> k_{-4} = k_{23}$).

We tested the possibility that two steps with different but individually constant activation energies could have given rise to the discontinuous temperature dependence of V_{so}. The best fit to the points calculated for log k_4C_t and $k_{23}C_t$, the components of V_{so}, was determined on the presumption of constant activation energies. The resulting values were reconverted into V_{so} values (not shown). The curve obtained was essentially similar to the best straight-line fit of the data generated by linear regression. The straight-line fit was not as good as the model with a discontinuity at 23 °C. The latter model fit the data with an r^2 of 0.98. This exercise demonstrated that the peculiar temperature dependence of net transport very likely arises from its rate-limiting step having an activation energy which changes abruptly at 23 °C and not from a combination of individually constant activation energies.

Carrier Distribution. In the absence of sugar, empty binding sites of some transporters will face inward and others will face outward at a given instant. The fraction facing either way depends on the ratio of empty-site reorientation coefficients, k_4/k_{-4}. Specifically, the fraction facing outward is $k_4/(k_4 + k_{-4})$ or $(k_4/k_{-4})/(k_4/k_{-4} + 1)$. At most temperatures (as seen in Figure 5 and elsewhere), k_4 is much less than k_{-4}, so most of the sugar-free sites face inward. The resistance plot can define the range of possible rate coefficient values and the range of possible ratios among them. In the example of Figure 5, the k_4/k_{-4} ratio at the left dotted line is 0.30, the k_4/k_{-4} ratio at the right dotted line is 0, and the k_4/k_{-4} ratio halfway in between is 0.13. The resistance plots from all experiments at all temperatures had this same general appearance. We

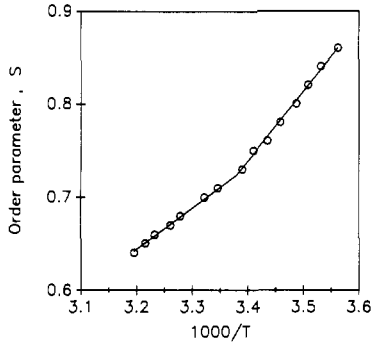

FIGURE 9: Temperature dependence of membrane lipid ordering using the spin probe 5-NS. A plot of the order parameter S (dimensionless; see Materials and Methods) for the spin probe 5-NS against $1000/T$ is shown. A piecewise regression was carried out confirming a discontinuity at $1000/T = 3.39$ (22 °C) with $r^2 = 0.996$.

calculated the fraction of empty carriers facing outward from k_4 and k_{-4} values at the left and middle of the range of possible k_4 values. The results are shown in Figure 8. Clearly, the vast majority of the carriers are facing inward at lower temperatures. It appears that the distribution becomes more even as temperature rises, because the slower step (k_4) is the more temperature-sensitive step.

Temperature Dependence of Lipid Ordering. The change in activation energy of k_4C_t could be associated with a phase change in the lipid environment of the cell membrane. To investigate this possibility, the temperature dependence of the ordering of membrane lipid was studied by using electron paramagnetic resonance spectroscopy and a fatty acid spin probe. The order parameter, S, provides an estimate of ordering of membrane lipids. As shown in Figure 9, S decreased monotonically from a value of 0.862 at 2 °C to 0.638 at 40 °C, indicating decreasing order of lipids with increasing temperature. Plots of S versus temperature were distinctly nonlinear with the most curvature in the 20–30 °C range. Fitting of the observed data, replotted as S versus $1000/T$, by piecewise linear regression of the data gave a good correlation ($r^2 = 0.996$) when the data were grouped about a breakpoint at 23 °C.

Activation Energies of Transport-Associated Phenomena. Activation energies (Table III) were calculated from the slopes of Figures 6, 7, and 8 according to the Arrhenius equation. The magnitude of the value indicates the relative difficulty of the step. The activation energies for k_4 and V_{so} were the highest, consistent with the fact that k_4 is the least facile step and V_{so} is largely governed by k_4. Activation energies for V_{so}, k_4, and V_{sb} were all substantially less above 23 °C than they were below 23 °C, as evident from the graphs.

Discussion

The transport of glucose across the plasma membrane of a mammalian cell is catalyzed by a transporter whose function involves four steps: binding of sugar on the cis side, conformational change of the sugar–carrier complex so that the bound sugar faces the trans side, dissociation of the bound sugar, and return of the empty binding site to the cis side (Widdas, 1952). The transport rate law contains four independent empirical coefficients, whose values reveal relations among the rate coefficients of the four steps (Regen & Morgan, 1964; Regen & Tarpley, 1974). In some cell types, the carrier is quite asymmetrical, in that analogous rate coefficients for various steps differ substantially. This property allows some of the step coefficients to be evaluated accurately while others can be estimated approximately (Whitesell et al., 1977a). In the case where regulation of glucose transport involves effects other than a simple change in the quantity of transporters, estimation of step coefficients and dissociation constants might provide insights as to the regulatory action.

The kinetic characteristics of glucose transport in the rat erythrocyte turn out to be simple but informative. The K_m and V_{max} of efflux were the same as those of equilibrium exchange over the range of temperatures tested. This was seen in simultaneous measurements of efflux and equilibrium exchange and was confirmed by the fact that the influx K_m was at all temperatures not affected by a fixed internal sugar concentration (i.e., $H_s = K_{so}$). These findings indicate either that outward movement of the loaded carrier is the rate-limiting step for both efflux and equilibrium exchange ($k_{23} \gg k_{-21} \ll k_{-4}$) or that the loaded and empty carriers move inward with the same ease ($k_{23} = k_{-4}$) or both ($k_{23} = k_{-4} \gg k_{-21}$).

Our data show the outward reorientation of empty carrier to be very slow compared to all other steps. This accounts for the fact that the K_m and V_{max} of entry (K_{so} and V_{so}) are much smaller than those of exit (K_{si} and V_{si}) and exchange (B_s and V_{sb}). The exit K_m (K_{si}) exceeds the entry K_m (K_{so}) because the dissociation constant of in-facing carrier (K_{sdi}) exceeds that of out-facing carrier (K_{sdo}). This could occur because the factor stabilizing in-facing empty carrier also interferes with sugar binding to the carrier.

The entry V_{max} (V_{so}) was much more sensitive to temperature than was the exit V_{max} (V_{si}) or the exchange V_{max} (V_{sb}). The entry V_{max} reflects almost exclusively the coefficient of the empty carrier's outward motion (k_4). Between 17 and 37 °C, k_4 and V_{so} increased about 44-fold, while V_{sb} and V_{si} increased about 8-fold. However, even at the highest temperatures, V_{so} was still less than half of V_{sb} or V_{si}. The exceptional temperature dependence of k_4 is consistent with a very low energy state of in-facing empty carrier. Some factor is stabilizing this form and imparting extra energy of activation as well as extra free energy to departures from this form (from C_i to C_o or to CS_i).

It is also interesting that the K_m's of exit and equilibrium exchange (K_{si} and B_s) are hardly affected by temperature while the K_ms of entry and counterflow (K_{so} and R_s) increase almost 5.5-fold from 17 to 37 °C. The increase of K_{so} with temperature probably represents the effect of heat to promote dissociation. This fundamental action affected K_{si} very little, possibly because it was masked by a concomitant effect to release in-facing empty carrier from a stabilizing factor which interferes with sugar binding.

An abrupt transition at 20 °C, in the activation energy for the entry (V_{so}) and exchange V_{max}'s (V_{sb}) of glucose transport in human RBC, has been reported by Lacko et al. (1973). In the present work with rat erythrocytes, a dramatic transition for V_{so} and k_4 was observed at 23 °C. A comparable transition occurred in Arrhenius plots of V_{si} (exit V_{max}) and V_{sb} (exchange V_{max}), though it was less impressive because these parameters were less temperature dependent and there was more variance in the measurement of V_{sb} than in the measurement of V_{so}.

Studies of membrane fluidity at various temperatures indicated that the break in activation energies for the transport steps discussed above could reflect a phase transition of membrane lipids. The spin-label probe used, 5-NS, inserts into the lipid bilayer with its alkyl chain containing the spin-label moiety intercalated between endogenous membrane lipid chains and with its carboxyl group located at the lipid–water interface. Thus, the label at the 5-carbon position provides a monitor of lipid ordering in a region just beneath the lipid–water interface. The plots of S versus $1/T$ suggest that there may be an alteration in the ordering of membrane

lipids near 23 °C, in agreement with results previously reported in human erythrocytes (Forte et al., 1985). The lipid to protein ratio in erythrocytes is sufficiently high to exclude the possibility of observing the relatively small proportion of membrane lipid in contact with membrane proteins (boundary lipid). Therefore, the results presented reflect the properties of the bulk lipid in the bilayer averaged over all environments accessible to the 5-NS probe. A correlation between membrane fluidity and transport activity has been suggested recently for the Ca-ATPase of sarcoplasmic reticulum (Bigelow & Thomas, 1987). It was shown that diethyl ether, which mobilizes membrane lipids, increases the rotational motion of the Ca-ATPase and increases enzymic activity. The results presented in this study illustrate a similar correlation between the effect of temperature on lipid fluidity and glucose transport activity in rat RBC. Furthermore, they suggest that the activation energy of the rate-limiting step in the transport cycle exhibits a sudden change around the transitional temperature for membrane lipids.

Recently there has been renewed interest in studying the intrinsic regulabilty of the glucose carrier in rat adipocytes, by catecholamines (Joost et al., 1986), for example. The adipocyte glucose transport system is reported by some (Vinten, 1984) but not all (Taylor & Holman, 1981) to be asymmetric.[2] This means that a step in the carrier cycle may be rate limiting and a probable site of any intrinsic regulation. Such intrinsic regulation of the glucose carrier would be expected to result in a change of its kinetic characteristics, which are complexes of various steps in the model. We reported that metabolic feedback changed the apparent K_m for glucose transport in the rat adipocyte. Regulation of the K_m by insulin and glucose metabolism was temperature dependent and observed at 37 °C but not at 23 °C (Whitesell & Abumrad, 1985, 1986). Changes in the transport K_m were also observed in thymocytes (Whitesell & Regen, 1978; Whitesell et al., 1977b). A recent report finds a major effect of insulin on the K_m of glucose transport in rat hindlimb (Ploug et al., 1987). All this suggests that regulation of glucose transport by changing the K_m of the transporter might be common to many cell types.

Glucose transport in the rat erythrocyte (Abumrad et al., 1988), similarly to that in adipocytes (Whitesell & Abumrad, 1986), thymocytes (Whitesell & Lynn, 1979), and Chinese hamster fibroblasts (Ullrey et al., 1982), is subject to feedback regulation by glucose metabolites, possibly including glucose 6-phosphate. When the cells are preincubated with glucose or deoxyglucose, a depression of transport activity can be observed. Nonphosphorylatable hexoses do not exert this inhibitory action. The inhibitory effect of preincubation with glucose is preserved after chilling, washing, and rewarming of the cells to assay at 40 °C, but it is not seen if the assay is done at 14 °C (Abumrad et al., 1988). Thus, regulation of glucose transport by glucose metabolism is temperature dependent, and understanding the effect of temperature on transport may provide insight as to the mechanism of this regulation. Study of glucose transport regulation in the rat red cell offers significant advantages at this stage. Red cells lack intracellular organelles, so their glucose transporters can be studied without the possibility of augmentation from intracellular stores, which is a possibility in adipocytes (Suzuki & Kono, 1980; Cushman & Wardzala, 1980) or muscle cells (Wardzala & Jeanrenaud, 1981). The scope of the present study was limited to estimating step coefficients and dissociation constants in the glucose transport cycle and their dependences on temperature. With some modifications and limitations, these techniques can be used to analyze the inhibitory effects of glucose metabolism on the transporter. This will help toward understanding the mechanism of action of transport-modulating agents in a simple cell, which may be applicable to more complex cells.

Registry No. Glucose, 50-99-7.

[2] R. R. Whitesell, and N. A. Abumrad, unpublished observations. We have observed asymmetry of efflux kinetics in the adipocyte.

References

Abumrad, N. A., Briscoe, P., Beth, A. H., & Whitesell, R. R. (1988) *Biochim. Biophys. Acta 938*, 222–230.

Amatruda, J. M., & Finch, E. D. (1979) *J. Biol. Chem. 254*, 2619–2625.

Bigelow, D. J., & Thomas, D. D. (1987) *J. Biol. Chem. 262*, 13449–13456.

Cushman, S. W., & Wardzala, L. J. (1980) *J. Biol. Chem. 255*, 4758–4762.

Ezaki, O., & Kono, T. (1982) *J. Biol. Chem. 257*, 14306–14310.

Forte, T., Leto, T. L., Minetti, M., & Marchesi, V. T. (1985) *Biochemistry 24*, 7876–7880.

Gaffney, B. J. (1976) in *Spin Labeling: Theory and Applications* (Berliner, L. J., Ed.) pp 567–571, Academic, Press, New York.

Hankin, B. L., & Stein, W. D. (1972) *Biochim. Biophys. Acta 288*, 127–136.

Joost, H. G., Weber, T. M., Cushman, S. W., & Simpson, I. A. (1986) *J. Biol. Chem. 261*, 10033–10036.

Lacko, L., Wittke, B., & Geck, P. (1973) *J. Cell. Physiol. 82*, 213–218.

Lowe, A. G., & Walmsey, A. R. (1986) *Biochim. Biophys. Acta 857*, 146–154.

Ploug, T., Galbo, H., Vinten, J., Jorgensen, M., & Richter, E. A. (1987) *Am. J. Physiol. 253*, E12–20.

Regen, D. M., & Morgan, H. E. (1964) *Biochim. Biophys. Acta 79*, 151–166.

Regen, D. M., & Tarpley, H. L. (1974) *Biochim. Biophys. Acta 339*, 218–233.

Suzuki, K., & Kono, T. (1980) *Proc. Natl. Acad. Sci. U.S.A. 77*, 2542–2545.

Taylor, L. P., & Holman, G. D. (1981) *Biochim. Biophys. Acta 642*, 325–335.

Ullrey, D. B., Franchi, A., Pouyssegur, J., & Kalckar, H. M. (1982) *Proc. Natl. Acad. Sci. U.S.A. 79*, 3777–3779.

Vinten, J. (1984) *Biochim. Biophys. Acta 772*, 244–250.

Wardzala, L. J., & Jeanrenaud, B. (1981) *J. Biol. Chem. 256*, 7090–7093.

Whitesell, R. R., & Regen, D. M. (1978) *J. Biol. Chem. 253*, 7289–7294.

Whitesell, R. R., & Lynn, W. S. (1979) *Fed. Proc., Fed. Am. Soc. Exp. Biol. 38*, 2621.

Whitesell, R. R., & Abumrad, N. A. (1985) *J. Biol. Chem. 260*, 2894–2899.

Whitesell, R. R., & Abumrad, N. A. (1986) *J. Biol. Chem. 261*, 15090–15096.

Whitesell, R. R., Tarpley, H. L., & Regen, D. M. (1977a) *Arch. Biochem. Biophys. 181*, 596–602.

Whitesell, R. R., Hoffman, L., & Regen, D. M. (1977b) *J. Biol. Chem. 252*, 3533–3537.

Widdas, W. F. (1952) *J. Physiol. 118*, 23–39.